Effect of Compounding Sequence on the Morphology of Organoclay-Filled PA6/PP/MAPP Blends

Li Wang, Zhao-Xia Guo, Jian Yu

Key Laboratory of Advanced Materials (MOE), Department of Chemical Engineering, Tsinghua University, Beijing 100084, People's Republic of China

Received 27 May 2010; accepted 12 September 2010
DOI 10.1002/app.33450
Published online 10 December 2010 in Wiley Online Library (wileyonlinelibrary.com).

ABSTRACT: Four types of compounding sequences were utilized to prepare organoclay-filled polyamide 6 (PA6)/polypropylene (PP)/maleic anhydride grafted PP (MAPP) blends. The amount of PA6 molecules grafted to MAPP during *in situ* compatibilization reaction and the distribution ratio of organoclay in the continuous phase and interface zone were determined quantitatively. The relationship among dispersion and distribution states of organoclay, the amount of PA6 grafted to MAPP as well as the deformation, breakup and coalescence of dispersed droplets was elucidated to interpret the difference in phase morphology. Crystallization behavior and dynamic mechanical properties were also investigated and correlated with the morphology of the materials. It has been shown that the PA6/organoclay masterbatch approach results in the smallest average domain size because of the best organoclay dispersion, the highest amounts of PA6 grafted to MAPP, and organoclay at the interface, which efficiently stabilizes the droplets and prevents coalescence of the droplets. The material prepared by this approach has the biggest improvement in dynamic storage modulus. © 2010 Wiley Periodicals, Inc. J Appl Polym Sci 120: 2261–2270, 2011

Key words: blends; organoclay; morphology; sequence; interaction

INTRODUCTION

Blending is a common way in tailoring the properties of polymeric materials. By blending two or more polymers, the advantages of different polymers can be combined and their respective shortcomings can be compensated, thus achieving balanced and optimized properties. However, the thermodynamic incompatibility of most polymers leads to phase separation and consequently poor mechanical properties. Special measures ought to be taken to improve the compatibility between polymers and obtain fine phase morphology. Traditionally, a block or graft copolymer which is synthesized prior to blending or forms *in situ* is utilized as compatibilizer.[1]

With the development of polymer nanocomposites, it has been found by many researchers that the incorporation of clay can bring about significant changes in blend morphology, causing the average domain size of sea-island structure to decrease[2–8] or increase.[9,10] The former case is frequently encountered and the mechanisms proposed to interpret this phenomenon include: (1) clay locates at the interface between two phases, acting like a compatibilizer by reducing interfacial tension and suppressing droplets coalescence[2,3]; (2) clay induces a drop in viscosity ratio of the dispersed phase to the continuous phase, promoting breakup of the dispersed droplets[7]; (3) clay acts as physical barrier preventing coalescence of the dispersed domains.[4]

For clay-filled polymer blends, compounding sequence often plays an important role in determining the phase morphology. González et al.[11] found that mixing organoclay with premixed PA6/mSEBS yielded finer phase morphology than mixing mSEBS with premixed PA6/organoclay for organoclay-filled PA6/mSEBS. The additionally improved compatibilization was attributed to a more effective reaction between the maleic groups of mSEBS and the amine end groups of PA6 by substituting the interaction between the surfactant of organoclay and mSEBS. Gallego et al.[12] prepared organoclay-filled PA6/mEPDM/EPDM-g-MA using four types of compounding sequences, and found that mixing all the components simultaneously or mixing organoclay with premixed PA6/mEPDM/EPDM-g-MA gave smaller average particle size than the other two compounding sequences. Zhang et al.[13] reported that mixing organoclay or PA6/organoclay with PA6/EPDM-g-MA preblends resulted in finer phase morphology than one-step mixing or mixing PA6/organoclay with EPDM-g-MA in the preparation of

Correspondence to: Z.-X. Guo (guozx@mail.tsinghua.edu.cn) or J. Yu (yujian03@mail.tsinghua.edu.cn).

TABLE I
Organoclay-Filled PA6/PP/MAPP Blends Prepared by Four Different Types of Compounding Sequences

Sample	First step	Second step
10–5D	Mixing PA6, PP, MAPP, and organoclay	
10–5M	Mixing PA6 and organoclay (9:1)	Mixing PA6/organoclay masterbatch with PA6, PP, and MAPP
10–5P	Mixing PP, MAPP, and organoclay	Mixing PP/MAPP/organoclay composite with PA6
10–5B	Blending PA6, PP, and MAPP	Mixing PA6/PP/MAPP blend with organoclay

PA6/EPDM-g-MA/organoclay nanocomposites, due to the avoidance of interaction between the surfactant of organoclay and EPDM-g-MA. Filippi et al.[14] found that adding organoclay to LDPE/PA6/SEBS-g-MA preblend at proper SEBS-g-MA/organoclay ratios gave significantly reduced domain size than mixing LDPE and PA6 with premixed SEBS-g-MA/organoclay. All the above-mentioned cases involve PA6 and maleinized polymer (as the traditional compatibilizer). The competitive interactions of PA6 and the surfactant of organoclay with the maleinized polymer were often mentioned to explain the difference in domain size in different compounding sequences. It seems that in all cases adding organoclay to the preblend of PA6/the second polymer/maleinized polymer gives the smallest particle size, because the reaction between PA6 and the maleinized polymer can be maximized if organoclay is added after preblending.

Polyamide 6 (PA6)/polypropylene (PP) is a typical blending system of interest from both academia and industry. There has been some research focusing on the influence of clay on the morphology of PA6/PP blends. Chow et al.[15–19] prepared both uncompatibilized and MAPP-compatibilized PA6/PP/clay nanocomposites by mixing all the components simultaneously and investigated morphology and mechanical and rheological properties. However, the effect of compounding sequence on the morphology of the final materials has not been considered. In this work, we investigate the effect of four types of compounding sequences on the morphology of organoclay-filled PA6/PP/MAPP blends. The amount of PA6 grafted to MAPP and the distribution of organoclay are determined quantitatively. A mechanism for morphology formation is proposed to interpret the difference in phase morphology for the four samples prepared by different compounding sequences. Crystallization behavior and dynamic mechanical properties are also characterized and correlated with morphology.

EXPERIMENTAL

Materials

PA6 (B3S, melting point: 220°C) was purchased from BASF Corp. PP (S1003, melting point: 165°C) was obtained commercially from China Petrochemical Co. Ltd. Maleic anhydride grafted PP (MAPP) with 1 wt % of MA was prepared by reactive extrusion in our laboratory. Organoclay (OMMT, CEC: 95 meq/100 g; gallery distance: 2 nm) was supplied by Zhejiang Huate Chemical Co., Ltd. under the trade name of NB901. It is a montmorillonite organically modified with a quaternary ammonium salt.

Preparation of organoclay-filled PA6/PP/MAPP blends

Organoclay-filled PA6/PP/MAPP blends were prepared using a torque rheometer (RM200A, Harbin Hapro Electrical Technology Co., Ltd.) at a temperature of 230°C and a screw speed of 60 rpm. The weight ratio of PA6/PP/MAPP/organoclay was 70/20/10/3.7. Methyl methacrylate (MMA) of equal weight to organoclay was added as cointercalation agent, according to our previous work.[20] This composition was designated as 10-5, in which the first number meant that the incorporation amount of MAPP was 10 wt % to all the polymers (PA6 + PP + MAPP) and the second number meant that the addition amount of organoclay was 5 wt % compared with PA6. Four types of compounding sequences were designed, named as D, M, P, and B, to prepare a series of 10-5 samples (Table I).

10-5D: All components were mixed Directly for 10 min. This compounding method is called direct mixing or one-step mixing.

10-5M: A Masterbatch rich in organoclay was first prepared by compounding PA6 with organoclay at a weight ratio of 9 : 1 for 10 min. Then desired amount of PA6/organoclay masterbatch, PA6, PP, and MAPP were compounded for another 10 min. This compounding method is called masterbatch approach.

10-5P: PP and MAPP were first compounded with organoclay at 180°C for 5 min and then the composite was blended with PA6 for another 10 min.

10-5B: PA6, PP, and MAPP were first Blended for 10 min and then compounded with organoclay for another 10 min. This compounding method is called preblending approach.

To investigate the morphology evolution, during the compounding process of 10-5D, 10-5M, and 10-5B, a small amount of melt was taken out from the chamber of torque rheometer at 2, 4, 7, and 10 min and immersed into cold water quickly to freeze

morphology evolution. Then, the PA6 matrix was removed by extraction with formic acid, and the residue was observed under FESEM.

The reference blends which don't contain organoclay (10-0) or both organoclay and MAPP (0-0) were also prepared by compounding all components directly at 230°C for 10 min with a screw speed of 60 rpm.

Removal of the continuous phase

The continuous phase (PA6) of all the samples was removed by solvent dissolution using formic acid. Solvent dissolution was assisted by magnetic stirring and lasted for 1 day, followed by centrifuging at a speed of 4000 rpm and recovering powder floating on top of the solution. Generally, this procedure was repeated four times to ensure complete removal of PA6 phase. PA6-g-PP formed through the reaction between the maleic groups of MAPP and the end amine groups of PA6[21] couldn't be dissolved. Thus, the recovered powder consisted of dispersed PP phase and the interface zone.

Characterization

Field emission scanning electron microscopy

Field emission scanning electron microscopy (FESEM) analysis was performed with a JEOL JSM-7401F apparatus operating at an accelerating voltage of 1 kV. The samples were cryo-fractured in liquid nitrogen. Particle size analysis of the dispersed phase was carried out using a JEOL software (smileview). The number average diameters of dispersed particles are defined as follows:

$$D_{\mathrm{av}} = \sum D_i / N$$

where D_i is the diameter of the ith dispersed particle and N is the total number of dispersed particles measured.

Transmission electron microscopy

Transmission electron microscopy (TEM) observation was conducted on a Hitachi H-800 transmission electron microscope at an accelerating voltage of 200 kV. Ultrathin slices were obtained using an cyroultratome (LKB model 2088; LKB-Producter AB, Bromma, Sweden) without staining.

Thermogravimetric analysis

To determine the distribution state of organoclay quantitatively, thermogravimetric analysis (TGA) (TA Instruments TGA2050) was conducted on the recovered PP/MAPP samples after extraction of PA6 by formic acid from ambient temperature to 600°C at a heating rate of 20°C/min in N_2 atmosphere. The weight percentage of organoclay in recovered PP/MAPP phase (W) was obtained from TGA. After the estimation of the amount of PA6 grafted to MAPP (shown below), the distribution ratio of organoclay in the PA6 phase and at the interface can be obtained.

Fourier transform infrared spectroscopy

The recovered PP/MAPP samples were melt-compressed into thin films and characterized with a NICOLET 560 Fourier transform infrared spectroscope (FTIR). organoclay was mixed with dry KBr and pressed into a pellet for infrared analysis. OMNIC software was utilized to determine the amount of PA6 grafted to MAPP. The spectra were processed as follows:

- Subtract the contribution of organoclay from IR spectrum (designated as S): all spectrum were normalized and subtraction was processed: $S_{\mathrm{sample}} - W^{*}S_{\mathrm{organoclay}}$.
- Estimating ${A_{1650\mathrm{cm}}}^{-1}/{A_{1370\mathrm{cm}}}^{-1}$ of the subtracted spectrum by integration, with ${A_{1650\mathrm{cm}}}^{-1}$ and ${A_{1370\mathrm{cm}}}^{-1}$ being the area of amide I band (characteristic absorption peak of PA6) and the bending vibration of C—H bond (characteristic absorption peak of PP).
- Determination of the amount of PA6 grafted to MAPP: the spectrum of PP/MAPP (at a weight ratio of 2 : 1) and PA6 were normalized and combined in such form: $S_{\mathrm{PP/MAPP}} - (-k)^{*}S_{\mathrm{PA6}}$. Different values of k were checked until the ${A_{1650\mathrm{cm}}}^{-1}/{A_{1370\mathrm{cm}}}^{-1}$ value of the combined spectrum was approximately equal to that in step 2. Then the amount of PA6 grafted to MAPP could be determined to be 30*k (the content of PP and MAPP in the blends was 30 wt %).

X-ray diffraction

The samples were compression molded into plates of approximately 1 mm thickness for X-ray diffraction (XRD) analysis, using a Rigaku D/max-RB diffractometer operating at 40 kV and 200 mA. The beam utilized was Cu Kα radiation with a wavelength of 1.5418 Å. Data were obtained in 2θ range from 1.5° to 10° at a scanning rate of 1°/min.

Differential scanning calorimetry

Differential scanning calorimetry (DSC) was carried out to study the nonisothermal crystallization and melting behavior of different samples using a Q100 calorimeter (TA Instruments). After annealing at

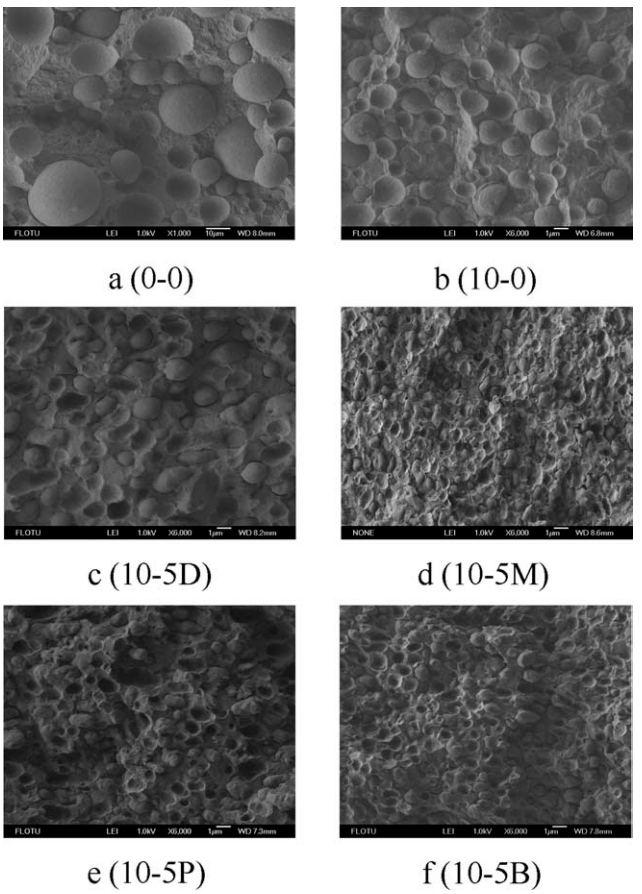

Figure 1 FESEM images of the reference blends (10-0 and 0-0) and organoclay-filled blends prepared by the four different types of compounding sequences. Magnification: ×1000 (a); ×6000 (b–f).

250°C for 5 min to eliminate any thermal history, samples were cooled to 50°C at a cooling rate of 10°C/min. Then samples were heated to 250°C at a heating rate of 10°C/min.

Dynamic mechanical analysis

All tested samples were melt-compressed into thin films at 235°C. Dynamic mechanical analysis (DMA) was performed in the temperature range from −100 to 100°C at a heating rate of 5°C/min, using a dynamic mechanical analyzer 2980 (TA Instruments). The frequency was 1 Hz and the strain was 20 μm.

RESULTS AND DISCUSSION

FESEM observation

Figure 1 shows FESEM images of all the samples prepared by the four different types of compounding sequences (10-5D, 10-5*M*, 10-5P, and 10-5B) along with the reference samples which do not contain organoclay (10-0) or both organoclay and MAPP (0-0). The average particle sizes for all the samples are listed in Table II. It can be seen that all the organoclay-filled PA6/PP/MAPP blends have smaller particle size than the reference sample without organoclay (10-0), indicating that organoclay can bring further reduction in particle size although the traditional compatibilizer MAPP has already significantly reduced the particle size (from 15.0 μm to 1.67 μm). The particle size order is 10-5M < 10-5B < 10-5P < 10-5D. The particle size of the sample prepared by preblending PA6/PP/MAPP approach (10-5B, 0.70 μm) is smaller than those of the samples prepared by direct mixing (10-5D, 1.24 μm) and premixing PP/MAPP/organoclay (10-5P, 1.00 μm). However, it is bigger than that of the sample prepared by PA6/organoclay masterbatch approach. It seems that similar PA6/organoclay masterbatch approach was not used for comparison in the related papers (Refs. [11–14]), although the method of premixing PA6/organoclay has been used.

TABLE II
Number Average Diameters of Dispersed Particles (D_{av}) for the Reference Blends (10–0 & 0–0) and Organoclay-Filled Blends Prepared by the Four Different Types of Compounding Sequences

Entry	0–0	10–0	10–5D	10–5M	10–5P	10–5B
D_{av} (μm)	15.0	1.67	1.24	0.45	1.00	0.70

Dispersion of organoclay

A combined means of XRD and TEM were used to investigate dispersion of organoclay in the blends prepared by the four different types of compounding sequences. The XRD patterns are shown in Figure 2. The original organoclay exhibits a broad peak at 2θ = 4.32°, corresponding to a gallery distance (*d*) of 2.05 nm. For samples 10-5M, a weak broad peak appears at about 2θ = 2.74 ° (*d* = 3.22 nm), indicating that organoclay was partially intercalated and partially exfoliated. The XRD patterns of 10-5D,

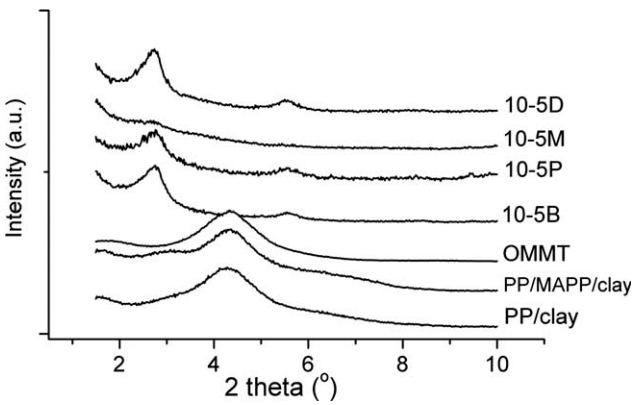

Figure 2 XRD curves of organoclay, PP/organoclay, PP/MAPP/organoclay, and organoclay-filled blends prepared by the four different types of compounding sequences.

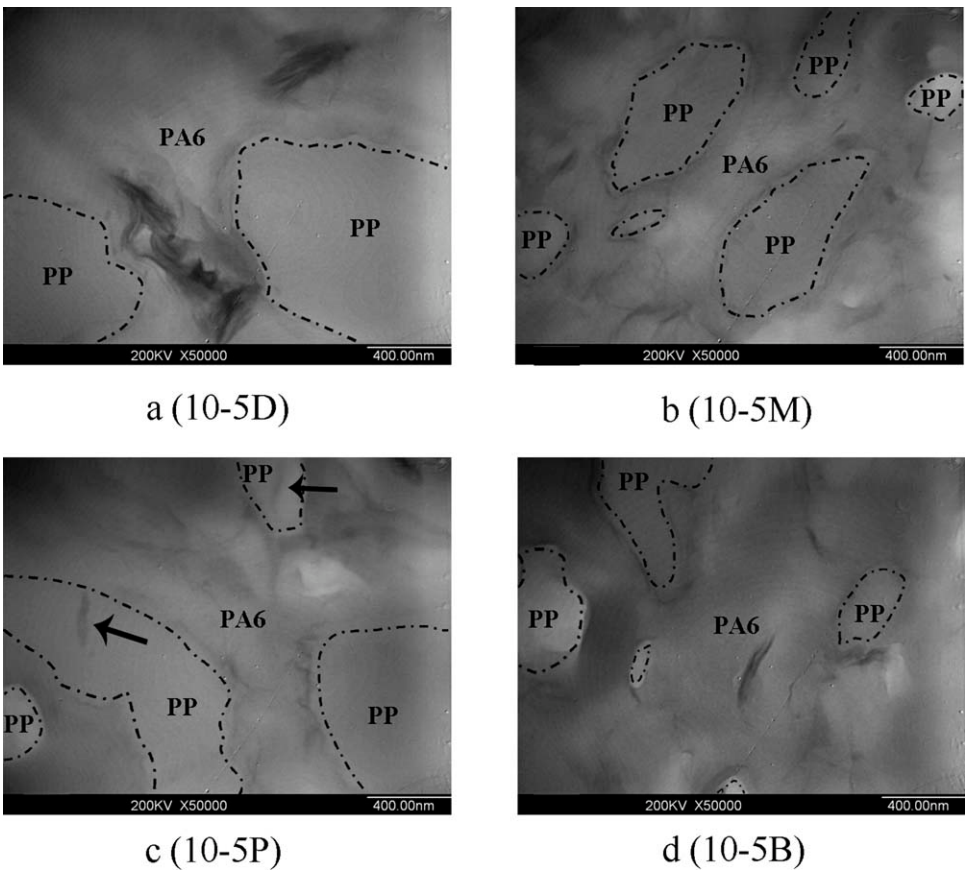

Figure 3 TEM images of organoclay-filled blends prepared by the four different types of compounding sequences.

10-5P, and 10-5B exhibit a strong peak at $2\theta = 2.74^\circ$ ($d = 3.22$ nm), which means that only intercalated state of organoclay was reached in these samples. Chow et al.[16] reported partial exfoliation of organoclay by direct mixing of all the components in a counter-rotating twin screw extruder for PA6/PP/MAPP/organoclay nanocomposites, while in our case only the PA6/organoclay masterbatch approach (10-5M) can reach partial exfoliation of organoclay. This difference may come from different compounding equipment and different source of organoclay and other components.

TEM images of all the samples (10-5D, 10-5M, 10-5P, 10-5B) are shown in Figure 3. To increase the phase contrast between polymer components and organoclay, no staining was conducted, which might cause weakened phase contrast between PA6 and PP. An overlay is drawn on TEM images to distinguish PA6 phase from PP phase. In samples 10-5D, 10-5M, and 10-5B, organoclay locates selectively in PA6 phase and at the interface, being basically in agreement with the results of Chow et al.[15] for the sample prepared by direct mixing in an extruder. Whereas for sample 10-5P, as pointed by the black arrows, intercalated organoclay was also observed in PP phase. Intercalation of MAPP into some of the organoclay galleries is possible when PP and MAPP were melt-mixed with organoclay, as evidenced by the appearance of the weak peak at $2\theta = 3.08^\circ$ ($d = 2.87$ nm) in the XRD pattern (Fig. 2).

Comparing the four images in Figure 3, it is recognized that the dispersion of organoclay is the worst in 10-5D, where large aggregates were observed, and the best in 10-5M where thin lines of organoclay platelets is shown.

Determination of the amount of PA6 grafted to MAPP

It is widely accepted that the maleic groups of MAPP can react with the end amine groups of PA6 molecules, forming a PA6-g-PP copolymer *in situ* at the interface which compatibilizes PA6/PP blends.[21] The amount of PA6 grafted to MAPP is a measure of the interaction level among the components and therefore an important factor affecting the degree of compatibilization, i.e., particle size, in the current PA6/PP/MAPP/organoclay system. The amounts of PA6 grafted to MAPP in all the four samples prepared by different compounding sequences were determined quantitatively by FTIR analysis of the residues after extraction of PA6 by formic acid. The spectra are shown in Figure 4. The characteristic absorption peaks of PA6, PP (MAPP) and

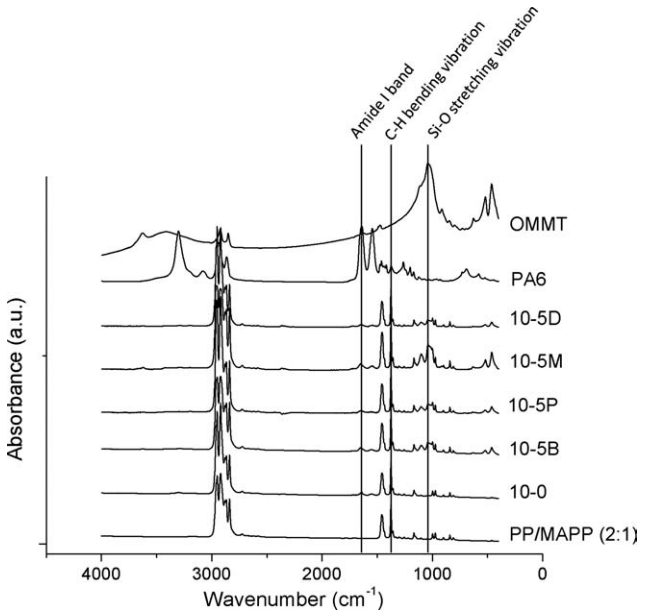

Figure 4 FTIR spectra of organoclay, PA6, PP/MAPP (2 : 1) and the recovered PP/MAPP phases of 10-5D, 10-5 *M*, 10-5P, and 10-5B.

organoclay show up at 1650 cm^{-1} (amide I band of PA6), 1377 cm^{-1} (bending vibration of C-H bond), and 1042 cm^{-1} (stretching vibration of Si-O bond), respectively. The amounts of PA6 grafted to MAPP were estimated to be 0.6, 1.5, 0.9, and 1.2 wt % to all the polymers for 10-5D, 10-5M, 10-5P, and 10-5B respectively, according to the area ratio of the peak at 1650 cm^{-1} to that at 1370 cm^{-1} which represents PA6/PP ratio. A rough estimation is made to evaluate the amount of end amine groups of PA6 available to react with MAPP. For the blending composition investigated in this work (PA6/PP/MAPP/organoclay = 70/20/10/3.7), 3.8 mmol of end amine groups in 70 g of PA6 (M_n = 18,000) will be available to react with about 1.0 mmol of MA groups in 10 g of MAPP (graft ratio: 1 wt %). It can be seen that the amount of PA6 molecules actually grafted to MAPP during compounding is very small compared to the theoretical value. This is due to the high molecular weight and high viscosity of the polymers, as well as limited interfacial area for compatibilization reaction to proceed. FTIR results imply that different compounding sequence yields different amount of PA6 grafted to MAPP, although the amounts of all the components used for compounding are exactly the same. By comparison, the amount of PA6 grafted to MAPP in decreasing order is: 10-5M > 10-5B > 10-5P > 10-5D, being in inverse order with the particle size. This is logical. Sample 10-5M has the largest amount of PA6 grafted to MAPP at the interface, meaning that the interaction among the components is the strongest, and therefore, the best compatibilization is achieved, leading to the smallest particle size. In the related literature work, the competitive interaction of PA6 and organoclay with MAPP was usually used to explain the relative amount of PA6-g-PP. It is hard to use this viewpoint to explain the current case: 10-5M > 10-5B. The difference in morphology evolution should be considered and will be discussed later.

Distribution of organoclay

The distribution of organoclay could be a very important factor affecting the role of organoclay in modifying the particle size, and it can be affected by the amount of PA6 grafted to MAPP at the interface. TEM images in Figure 3 only reveal the distribution state of organoclay qualitatively. The distribution of organoclay in the PA6 phase and at the interface was estimated by TGA analysis of the recovered residue (PP/MAPP) after extraction of PA6 by formic acid, which represents the amount of organoclay at the interface because there is no any organoclay in the PP phase except for sample 10-5P where a small amount of organoclay was found in the PP phase. The rest of organoclay is in the PA6 phase. The amounts of organoclay at the interface were 21%, 66%, 33%, and 38% for samples 10-5D, 10-5M, 10-5P, and 10-5B, respectively. The distribution of organoclay is correlated with the amount of PA6 grafted to MAPP in Figure 5 for the four samples prepared by different compounding sequences. It can be seen that the amount of organoclay distributed at the interface increase with increasing amount of PA6 grafted to MAPP. A straight line was drawn crossing point (0.6, 21) of 10-5D and point (0, 0) for comparison. 10-5P and 10-5B are around the line, while

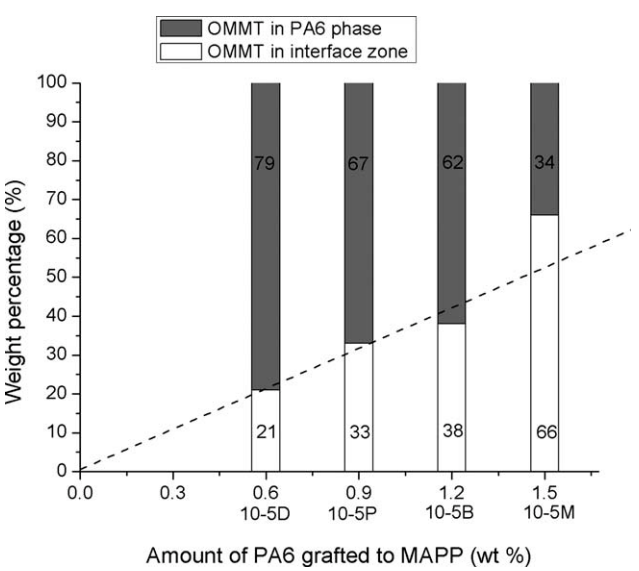

Figure 5 Relationship between the amount of PA6 grafted to MAPP and distribution ratio of organoclay in PA6 phase and interface zone.

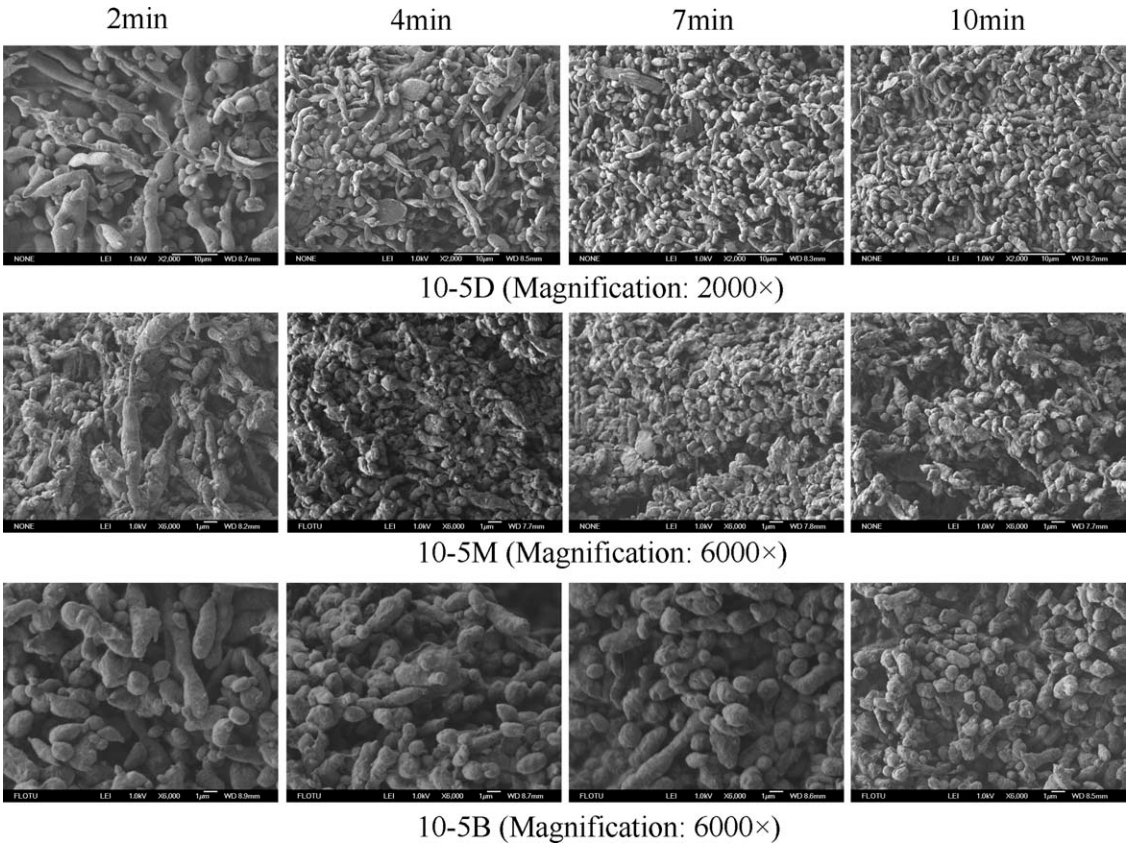

Figure 6 FESEM images of the recovered PP/MAPP phases for 10-5D, 10-5*M*, and 10-5B after 2, 4, 7, and 10 min of mixing.

10-5M lies above this line, indicating that more organoclay locates at the interface in 10-5M than that predicted by the straight line. This is because PA6 molecules are already intercalated into organoclay galleries before mixing with PP and MAPP. During the second mixing step, the end amine groups of PA6 molecules reacted with MAPP, forming PA6-g-PP copolymer or formed physical entanglement with MAPP molecules, bring many PA6-intercalated organoclay platelets to the interface due to its strong interaction with PA6.

Mechanism of morphology formation

The morphology evolution was investigated by observing the dispersed phase isolated after extraction of PA6 by formic acid at different time intervals. Figure 6 illustrates the morphology evolution process for samples 10-5D, 10-5M, and 10-5B. For both 10-5D and 10-5M, morphology evolution follows a transient mechanism of thread breakup.[22] Long fibrils were formed at 2 min in both cases, but the fibrils of 10-5D was much coarser than that of 10-5M. Therefore, the dispersion of PP phase in PA6 for 10-5M was more effective than that for 10-5D from the very beginning of mixing. As mixing time prolonged, the fibrils broke up into small droplets due to interfacial instabilities. Sample 10-5B was based on premixed blend of PA6/PP/MAPP, in which D_{av} was about 1.67 μm. After the incorporation of organoclay, dispersed droplets endured limited deformation and breakup, probably following a stepwise breakup mechanism,[22] and finally an equilibrium state ($D_{av} = 0.70$ μm) was reached.

The scheme in Figure 7 is proposed to interpret the mechanism of morphology, evolution, and morphological difference among samples prepared using different types of compounding sequences. For different compounding sequences, the initial distribution and dispersion states of organoclay are different, which influences droplets deformation and breakup at early stage of mixing through viscosity change and barrier effect of organoclay platelets. The initial droplets deformation and breakup is quite important because it determines the surface area exposed for compatibilization reaction, thus the amount of PA6 grafted to MAPP. PA6-g-PP in turn influences morphology evolution by reducing interfacial tension and suppressing droplets coalescence. Also, during compatibilization reaction, a certain amount of organoclay migrates and is immobilized to the interface due to its interaction with PA6-g-PP. This mechanism takes effect until an equilibrium state is reached.

Sample 10-5M has smaller particle size than 10-5B for the following reasons: (1) As discussed above, the morphology evolution is different in the two

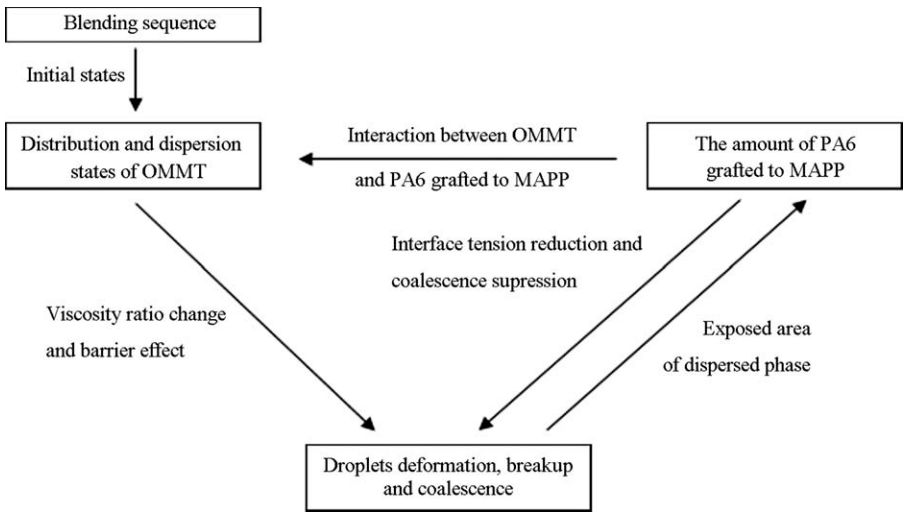

Figure 7 Scheme illustrating mechanism of morphology evolution.

cases. In the masterbatch approach (10-5M), organoclay was initially dispersed in PA6 and intercalated by PA6, promoting the initial deformation and breakup of PP phase. While in the preblending approach (10-5B), it took time for organoclay to be intercalated by PA6 molecules, being unfavorable for breakup of the preformed dispersed droplets. As shown in Figure 6, the particle size at 2 min of mixing for 10-5M is much finer than that for 10-5B. (2) The amount of PA6 grafted to MAPP is much higher in 10-5M than in 10-5B, leading to better compatibilization. (3) The amount of organoclay at the interface is much higher in 10-5M than in 10-5B, therefore the barrier effect is more efficient in 10-5M than in 10-5B. All these three reasons favor reduction in particle size for 10-5M.

As for 10-5D and 10-5P, organoclay located in PP phase initially (in 10-5D, PP melted first and organoclay went into PP before melting of PA6), which was unfavorable for the initial breakup of the dispersed phase. The amounts of both PA6 grafted to MAPP and organoclay distributed at the interface were much less than in the other two cases, leading to poor compatibilization and poor barrier effect of organoclay, and thus larger D_{av}. The D_{av} of 10-5P was a little smaller than that of 10-5D because of the better dispersion state of organoclay, slightly bigger amounts of PA6 grafted to PP and organoclay at the interface.

Crystallization behavior

The DSC cooling curves of all the samples prepared by the four different compounding sequences along with the reference sample 10-0, which does not contain organoclay, and PP are shown in Figure 8. The DSC curve of 10-0 exhibits two peaks at 122.49 and 193.27°C, corresponding to the crystallization of PP and PA6, respectively. The addition of organoclay shifts the crystallization peak of PA6 slightly, no matter which blending sequence was used. It is known that clay can either have a heterogeneous nucleation effect on polymer crystallization, causing an increase in crystallization temperature[23] or exert an opposite effect on polymer crystallization due to the hindrance of the diffusion of polymer chains towards crystal growth front by clay.[24] In our case, the latter effect seems to dominate over the former one in the crystallization of PA6.

The crystallization peak of PP in 10-0 (122.49°C) is higher than that in virgin PP (113.38°C), showing nucleation effect of PA6 on the crystallization of PP, although this effect is somehow diminished by MAPP.[25] In the presence of organoclay, the crystallization peak of PP splits into two peaks with the

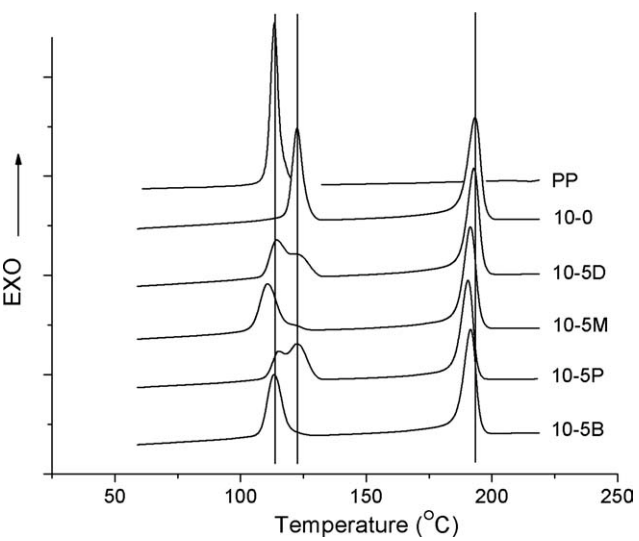

Figure 8 DSC cooling curves of PP, reference blend 10-0 and organoclay-filled blends prepared by the four different types of compounding sequences.

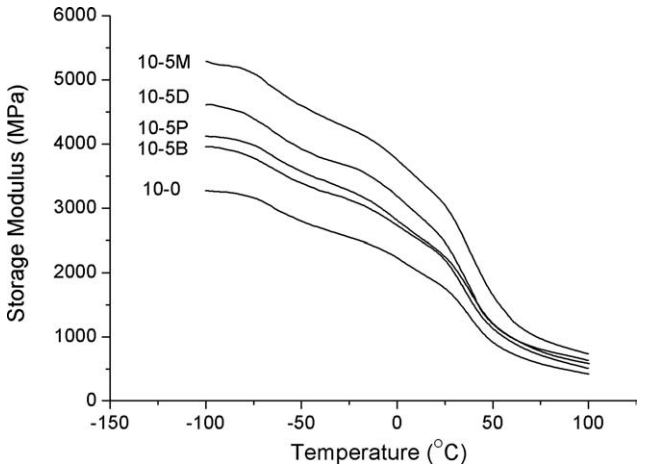

Figure 9 Dynamic storage modulus of reference blend 10-0 and organoclay-filled blends prepared by the four different types of compounding sequences.

appearance of a lower temperature peak for 10-5D and 10-5P, or shifted to a lower temperature for 10-5M and 10-5B. It is suspected that organoclay at the interface could shield the nucleation effect of PA6 in the crystallization of PP to some degree, similar to MAPP. When the amount of organoclay distributed at the interface reached a certain value, the high temperature peak was hardly noticeable (10-5M and 10-5B), indicating a complete shielding of the nucleation effect of PA6. The crystallization peak of PP in 10-5M is even lower than that in pure PP, indicating that organoclay not only shields the nucleation effect of PA6, but also hinders the diffusion of PP molecules to crystallization front, probably due to better dispersion state of organoclay.

Dynamic mechanical properties

The curves of dynamic storage modulus versus temperature for all the investigated organoclay-filled blends along with the reference sample 10-0 which does not contain organoclay are shown in Figure 9. The storage moduli of all organoclay-filled blends are higher than that of the reference blend. This reinforcing effect is especially prominent at low temperature (−100°C). The improvement in storage modulus for sample 10-5M prepared by PA6/organoclay masterbatch approach is outstanding compared to other samples. At 25°C its storage modulus was about 1.7 times of that of 10-0, while those of the others are only less than 1.4 times of that of 10-0. The storage modulus of polymer blends is mainly determined by the continuous phase, while dispersed phase and interface play a secondary role. The highest storage modulus of 10-5M is mainly attributed to good dispersion of organoclay in the PA6 phase. The smallest D_{av} (thus more interfacial area) and good interfacial strength may also have some contribution.

CONCLUSIONS

In this article, the effects of compounding sequence on the morphology, crystallization behavior and dynamic mechanical properties of organoclay-filled PA6/PP/MAPP blends have been investigated. Four types of compounding sequences were utilized. The following conclusions can be drawn:

1. Using PA6/organoclay masterbatch approach achieves the smallest average particle size. Quantitative analyses showed that the sample prepared by masterbatch approach has the highest amount of PA6 grafted to MAPP and organoclay at the interface. The difference in particle size was discussed using the proposed mechanism for morphology formation, considering the relationship among dispersion and distribution states of organoclay, the amount of PA6 grafted to MAPP as well as the deformation, breakup, and coalescence of the dispersed droplets.
2. Organoclay has no nucleating effect on crystallization of both PA6 and PP in all four compounding sequences. The crystallization peak of PA6 slightly lowers for all the samples, while that of PP either shows two peaks with appearance of a lower temperature peak or shifted to lower temperature due to presumably the hindrance of macromolecular chain diffusion towards crystal growth and shielding of the nucleation effect of PA6 to PP by the presence of organoclay at the interface.
3. The use of organoclay in the preparation of PA6/PP/MAPP blends can increase dynamic storage modulus no matter which compounding sequence is used. The material prepared by PA6/organoclay masterbatch approach exhibits the highest dynamic storage modulus, which is mainly attributed to the best dispersion state of organoclay in the PA6 phase.

References

1. Bucknall, C. B. Toughened Plastics; Applied Science Publishers: London, 1977.
2. Wang, Y.; Zhang, Q.; Fu, Q. Macromol Rapid Commun 2003, 24, 231.
3. Gelfer, M. Y.; Song, H. H.; Liu, L. Z.; Hsiao, B. S.; Chu, B.; Rafailovich, M.; Si, M. Y.; Zaitsev, V. J Polym Sci Part B: Polym Phys 2003, 41, 44.
4. Khatua, B. B.; Lee, D. J.; Kim, H. Y.; Kim, J. K. Macromolecules 2004, 37, 2454.
5. Dharaiya, D. P.; Jana, S. C. J Polym Sci Part B: Polym Phys 2005, 43, 3638.
6. Ray, S. S.; Bousmina, M. Macromol Rapid Commun 2005, 26, 450.
7. Ray, S. S.; Bousmina, M.; Maazouz, A. Polym Eng Sci 2006, 46, 1121.
8. Fang, Z. P.; Xu, Y. Z.; Tong, L. F. Polym Eng Sci 2007, 47, 551.

9. González, I.; Eguiazábal, J. I.; Nazábal, J. Compos Sci Technol 2006, 66, 1833.
10. Kontopoulou, M.; Liu, Y. Q.; Austin, J. R.; Parent, J. S. Polymer 2007, 48, 4520.
11. González, I.; Eguiazábal, J. I.; Nazábal, J. Eur Polym J 2008, 44, 287.
12. Gallego, R.; García-López, D.; López-Quintana, S.; Gobernado-Mitre, I.; Merino, J. C.; Pastor, J. M. J Appl Polym Sci 2008, 109, 1556.
13. Zhang, L. Y.; Wan, C. Y.; Zhang, Y. Polym Eng Sci 2009, 49, 209.
14. Filippi, S.; Dintcheva, N. T.; Scaffaro, R.; Mantia, F. P. L.; Polacco, G.; Magagnini, P. Polym Eng Sci 2009, 49, 1187.
15. Chow, W. S.; Ishak, Z. A. M.; Karger-Kocsis, J.; Apostolov, A. A.; Ishiaku, U. S. Polymer 2003, 44, 7427.
16. Chow, W. S.; Ishak, Z. A. M.; Ishiaku, U. S.; Karger-Kocsis, J.; Apostolov, A. A. J Appl Polym Sci 2004, 91, 175.
17. Kusmono, Z. A.; Ishak, Z. A. M.; Chow, W. S.; Takeichi, T. Rochmadi Express Polym Lett 2008, 2, 655.
18. Chow, W. S.; Ishak, Z. A. M.; Karger-Kocsis, J. J Polym Sci Part B: Polym Phys 2005, 43, 1198.
19. Chow, W. S.; Ishak, Z. A. M.; Karger-Kocsis, J. Macromol Mater Eng 2005, 290, 122.
20. Yang, Q. Q.; Guo, Z. X.; Yu, J. J Appl Polym Sci 2008, 108, 1.
21. Sathe, S. N.; Devi, S.; Rao, G. S. S.; Rao, K. V. J Appl Polym Sci 1996, 61, 97.
22. Janssen, J. M. H.; Meijer, H. E. H. J Rheol 1993, 37, 597.
23. Kang, X.; He, S. Q.; Zhu, C. S.; Lǔ, L. W. L.; Guo, J. G. J Appl Polym Sci 2005, 95, 756.
24. Homminga, D. S.; Goderis, B.; Mathot, V. B. F.; Groeninckx, G. Polymer 2006, 47, 1630.
25. Marco, C.; Ellis, G.; Gómez, M. A.; Fatou, J. G.; Arribas, J. M.; Campoy, I.; Fontecha, A. J Appl Polym Sci 1997, 65, 2665.